JOURNAL OF VIROLOGY, Apr. 2001, p. 3925–3936 Vol. 75, No. 8
0022-538X/01/$04.00+0 DOI: 10.1128/JVI.75.8.3925–3936.2001

Sequence Requirements for Interaction of Human Herpesvirus 7 Origin Binding Protein with the Origin of Lytic Replication

LAURIE T. KRUG,[1,2] NAOKI INOUE,[2] AND PHILIP E. PELLETT[1,2]*

Microbiology and Molecular Genetics Program, Emory University,[1] and Centers for Disease Control and Prevention,[2] Atlanta, Georgia

Received 24 October 2000/Accepted 24 January 2001

As do human herpesvirus 6 variants A and B (HHV-6A and -6B), HHV-7 encodes a homolog of the alphaherpesvirus origin binding protein (OBP), which binds at sites in the origin of lytic replication (*ori*Lyt) to initiate DNA replication. In this study, we sought to characterize the interaction of the HHV-7 OBP (OBP_{H7}) with its cognate sites in the 600-bp HHV-7 *ori*Lyt. We expressed the carboxyl-terminal domain of OBP_{H7} and found that amino acids 484 to 787 of OBP_{H7} were sufficient for DNA binding activity by electrophoretic mobility shift analysis. OBP_{H7} has one high-affinity binding site (OBP-2) located on one flank of an AT-rich spacer element and a low-affinity site (OBP-1) on the other. This is in contrast to the HHV-6B OBP (OBP_{H6B}), which binds with similar affinity to its two cognate OBP sites in the HHV-6B *ori*Lyt. The minimal recognition element of the OBP-2 site was mapped to a 14-bp sequence. The OBP_{H7} consensus recognition sequence of the 9-bp core, BRTYCWCCT (where B is a T, G, or C; R is a G or A; Y is a T or C; and W is a T or A), overlaps with the OBP_{H6B} consensus YGWYCWCCY and establishes YCWCC as the roseolovirus OBP core recognition sequence. Heteroduplex analysis suggests that OBP_{H7} interacts along one face of the DNA helix, with the major groove, as do OBP_{H6B} and herpes simplex virus type 1 OBP. Together, these results illustrate both conserved and divergent DNA binding properties between OBP_{H7} and OBP_{H6B}.

Human herpesvirus 7 (HHV-7) is a widely prevalent betaherpesvirus with an in vitro tropism for $CD4^+$ T lymphocytes (reviewed in reference 5). HHV-7 is usually acquired during early childhood after HHV-6 infection and is likely transmitted via saliva (29). HHV-7 has been associated with febrile illnesses in children, neurological manifestations during primary infection, and clinical complications in organ transplant patients.

The betaherpesvirus subfamily consists of the cytomegaloviruses and the roseoloviruses (HHV-7 and HHV-6 variants A and B [HHV-6A and HHV-6B]). Their genomes are genetically colinear, with origins of lytic replication (*ori*Lyts) in analogous positions upstream from U41, the gene encoding the major DNA binding protein (1, 7, 11, 23, 27). However, sequence features of their *ori*Lyt regions indicate substantial differences between cytomegaloviruses and roseoloviruses in their mechanisms for initiating viral replication. The minimal *ori*Lyt regions of the cytomegaloviruses are long (>1.3-kb) complex structures consisting of multiple inverted and direct repeats, in addition to numerous transcription factor recognition sites that are believed to mediate activation of the replication origin (2, 20, 21, 28). Unlike the cytomegaloviruses, *ori*Lyts of HHV-6A and HHV-6B have features in common with the replication origins of alphaherpesviruses; these origins are less complex and are centered around binding sites for a virus-encoded replication initiator protein, the OBP.

Roseoloviruses each encode a homolog of the alphaherpesvirus OBP (14, 16, 23), which has no homolog in the cytomegaloviruses. The most extensively characterized alphaherpesvirus OBP, herpes simplex virus type 1 (HSV-1) OBP (OBP_{H1}), binds as a dimer at each of two sites in its origins of replication (Box sites I and II in each ori_S and two Box I sites in ori_L) (17). Homodimer interactions at each box site are believed to lead to local DNA bending of the intervening AT-rich element, unwinding of the region in association with the single-stranded DNA binding protein, and recruitment of the viral replication machinery (6).

Like OBP_{H1}, the OBP of HHV-6B (OBP_{H6B}) binds two sites (OBP-1 and OBP-2) that flank an AT-rich spacer element in the minimal core of the *ori*Lyt region (14). The consensus recognition sequence differs between OBP_{H6B} and OBP_{H1}, and they are unable to bind each other's OBP site (15). OBP_{H7} and OBP_{H6B}, encoded by the U73 gene in each virus, share 58% amino acid identity, in contrast to their respective 32 and 31% identities with the more distantly related OBP_{H1} (23). Although the HHV-7 genome is generally well conserved with respect to HHV-6A and HHV-6B, there is little sequence similarity in the origin regions (reference 27 and data not shown). Nonetheless, van Loon et al. demonstrated that an HHV-6 *ori*Lyt-containing plasmid could replicate in HHV-7-infected cells (27). In addition, they found that mutation of the only site in the HHV-7 *ori*Lyt region that matches the OBP_{H6B} consensus recognition sequence resulted in the loss of transient plasmid replication in HHV-7-infected cells. Although these results indicate that OBP_{H7} may recognize sequences similar to those in the HHV-6 *ori*Lyt, they suggest that there are OBP sites in the HHV-7 *ori*Lyt that do not conform to the OBP_{H6B} consensus. Recognizing the limits of relying on the consensus sequence of a distinct, albeit closely related, herpesvirus to predict OBP_{H7}-binding sites, we have used a direct biochemical approach for their identification.

In this study, we characterized the interaction of OBP_{H7} with its cognate *ori*Lyt to better understand the initiation

* Corresponding author. Mailing address: Centers for Disease Control and Prevention, 1600 Clifton Rd., G18, Atlanta, GA 30333. Phone: (404) 639-2186. Fax: (404) 639-0049. E-mail: ppellett@cdc.gov.

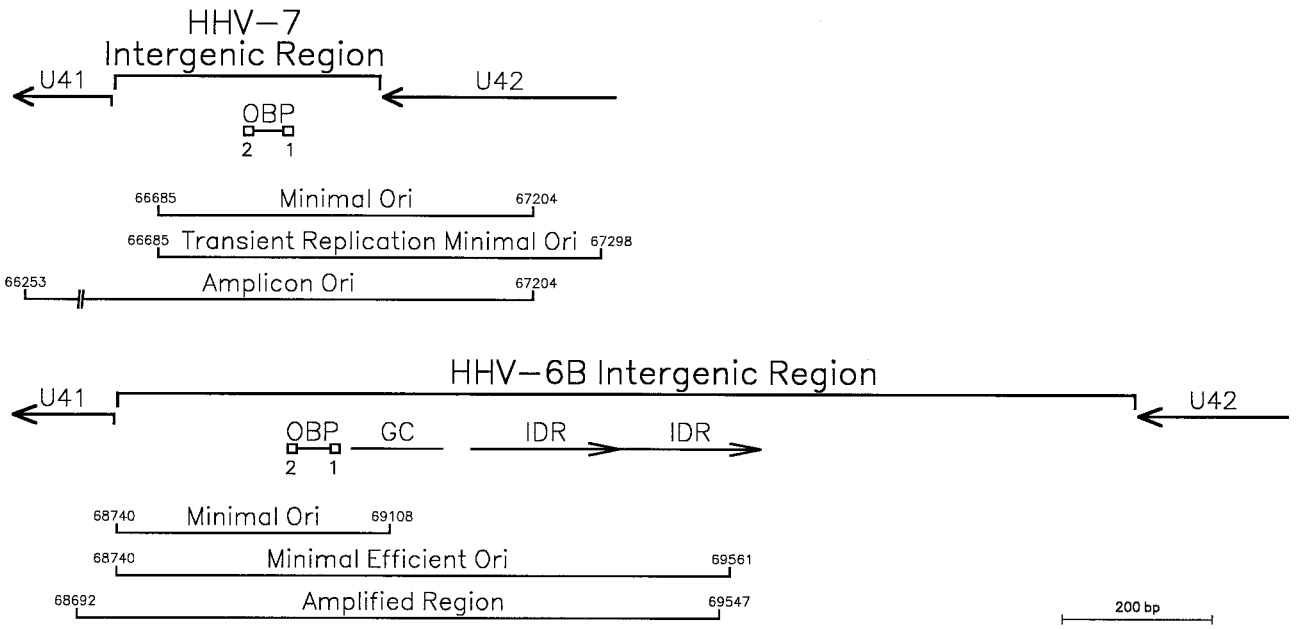

FIG. 1. The *ori*Lyt regions of HHV-7 and HHV-6B. The HHV-7 minimal origin as defined from plasmid (27) and amplicon (24) constructs includes two OBP sites flanking an AT-rich spacer element (described in this report). The HHV-6B minimal efficient origin determined by transient replication analysis (7) and a region found amplified in some cell culture passages of HHV-6B(Z29) (26) contains a G+C-rich region and IDRs to the right of the OBP sites. Coordinates are derived from HHV-7(RK) and HHV-6B(Z29).

mechanism of HHV-7 DNA replication. We found that in the HHV-7 *ori*Lyt, OBP_{H7} binds to two sites that flank an AT-rich spacer, and we studied its sequence and spatial binding requirements.

MATERIALS AND METHODS

RNA preparation and RT-PCR analysis. For mRNA studies, HHV-7(SB) was propagated in SupT1 cells as previously described (4). Total RNA was prepared from 10^6 SupT1 cells 7 days postinfection with HHV-7(SB) with a High Pure RNA isolation kit (Roche, Indianapolis, Ind.) according to the manufacturer's protocol. One microgram of RNA (extracted from approximately 1.5×10^5 cells) was treated with DNase (Roche) at 37°C for 30 min according to the manufacturer's recommendations. Twenty nanograms of DNase-treated RNA was reverse transcribed from oligo(dT) primers in a 40-μl reaction mixture by using a GeneAmp RNA PCR kit (PE Biosystems, Foster City, Calif.) according to the manufacturer's protocol. Ten microliters of the reverse transcriptase (RT) reaction mixture was then used for PCR analysis using primers specific for HHV-7 U73 (CCGAATCAAAACATTTACTCTA and AATCCGCTCTAATAGATTC TGCTA) and for the cellular gene glyceraldehyde-3′-phosphate dehydrogenase (GAPDH) (Stratagene, La Jolla, Calif.). Thermal cycling conditions were as follows: 35 cycles of 96°C for 15 s, 60°C for 30 s, and 68°C for 30 s with an increased extension of 5 s per cycle.

Plasmid construction. U73 fragments encoding the carboxyl-terminal portions of OBP_{H7} were amplified from HHV-7(SB) nucleocapsid DNA using a proofreading DNA polymerase (*Pfx*; GIBCO BRL, Rockville, Md.). Primers used were as follows: for the construct without a Kozak sequence, CGCGGATCCA TG**AACGGAGAATTCTA** and CCGGATATC**CGTTATGAACGCAATA**; and for constructs containing a Kozak consensus sequence surrounding the ATG, CGC ATCACG*GGATCC*GCCACCATG**GACGGAGAATTCTA** and CCG*GATATC***C GTTATGAACGCAATA** (restriction endonuclease sites used for cloning are italicized, residues in boldface indicate U73-derived nucleotides, and underlined ATG sequences were inserted for translation initiation). Using standard cloning techniques, these amplimers were digested, purified, and then ligated into the *Eco*RV site of pcDNA3 (Invitrogen, Carlsbad, Calif.) for the non-Kozak primer set or the *Bam*HI and *Eco*RV sites of pcDNA3 and pCMV-Tag 2B (Stratagene) for the Kozak-containing primer set. pCMV-Tag 2B provides a FLAG epitope tag at the amino terminus of the protein. A negative control pcDNA3-derived construct was also generated that contained U73 in the reverse orientation.

OBP_{H7} in vitro expression. OBP was expressed in coupled in vitro transcription-translation (IVTT) reactions (Promega, Madison, Wis.) as previously described with 2 μg of input DNA and 55% reticulocyte lysate (14). Negative control lysate was generated by programming the reactions with a plasmid containing U73 in the reverse orientation. ^{35}S-labeled in vitro-translated products were mixed with loading buffer and separated by sodium dodecyl sulfate-polyacrylamide gel electrophoresis as previously described (14).

Electrophoretic mobility shift analysis (EMSA). Oligonucleotides were annealed, labeled, and purified as described previously (14). DNA was incubated at room temperature for 20 min in 10 μl of either reaction buffer A or B with 2 μl of programmed IVTT lysate. Reaction buffer A consisted of 12 mM HEPES-NaOH (pH 7.6), 4 mM Tris-HCl (pH 7.6), 125 mM NaCl, 1 mM EDTA, 5 mM $MgCl_2$, 1 mM dithiothreitol, 120 μg of bovine serum albumin per ml, 12% glycerol, 5 μg of salmon testes DNA per ml, and a cocktail of protease inhibitors (Complete Mini EDTA-free; Roche). Buffer B (14) was similar to buffer A except that it contained 50 mM NaCl and no $MgCl_2$. DNA-protein complexes were separated in 5% polyacrylamide gels (60:1 acrylamide:*bis*-acrylamide) by using a low-ionic-strength electrophoresis buffer (14) at 4°C.

For competitive EMSA, reactions were set up as described above except that unlabeled competitor DNA was incubated with the lysate for 10 min at room temperature before the addition of the labeled target DNA. The percentage of binding inhibition was calculated by dividing the difference between the amount of signal in the absence and presence of competitor oligonucleotides by the amount of signal without competitor and then multiplying by 100. The percentage of wild-type inhibition was calculated by dividing the percentage of binding inhibition of the mutated competitor oligonucleotides by the percentage of binding inhibition of the wild-type oligonucleotide and then multiplying by 100. The percentage of oligonucleotide 7–2, L6R7, or 7–2B inhibition was calculated similarly. For supershift experiments, monoclonal antibodies (MAbs) against the FLAG (Stratagene) or the Xpress (Invitrogen) epitopes were incubated with the protein-DNA complexes for an additional 10 min at room temperature.

RESULTS

The HHV-7 *ori*Lyt region. As for the whole genome, the HHV-7 U41-U42 intergenic region is more compact than those of HHV-6A and HHV-6B (Fig. 1). The approximately 600-bp HHV-7 *ori*Lyt region mapped in transient replication

assays is composed of nearly all of the U41-U42 intergenic region and extends 300 bases into U42 (27). HHV-7 amplicons constructed by Romi et al. (24) utilized an approximately 1-kb *ori*Lyt region that extended only 200 bases into U42; this suggests that the minimal *ori*Lyt may be as short as 500 bp.

The 500-bp minimal HHV-7 *ori*Lyt shares little sequence similarity with the HHV-6 *ori*Lyts; it is one of the most divergent regions between the genomes of these viruses (data not shown). As illustrated in Fig. 1, within the 817-bp HHV-6B *ori*Lyt region is a 400-bp minimal essential domain that contains two OBP-binding sites flanking an AT-rich spacer element. Replication efficiency is enhanced by adjacent sequences that include a GC-rich segment and a putative DNA unwinding element within the AT-rich imperfect direct repeats (IDRs) of 187 and 192 bp (7, 18, 26). The HHV-6A *ori*Lyt region has a similar structure with an approximate 91% sequence identity to the homologous HHV-6B region, except there are three copies of an IDR that is related to, but shorter than, that in HHV-6B (8, 11). The minimal HHV-7 *ori*Lyt is not marked by the striking GC- and AT-rich regions of the HHV-6 *ori*Lyts and has no structures that correspond to the long IDRs or putative DNA unwinding elements found in the HHV-6A and HHV-6B *ori*Lyt regions (8, 27). Within the otherwise divergent HHV-7 *ori*Lyt, one site (OBP-2) is identical to the HHV-6 OBP-2 site and a second site (OBP-1) contains seven of nine matches to the OBP_{H6} consensus recognition sequence (15); these sites flank a 50-bp AT-rich element in the HHV-7 *ori*Lyt (Fig. 1) and have an overall structure that is similar to the lytic origin regions of HHV-6A, HHV-6B, and most alphaherpesviruses. These are the OBP_{H7}-binding sites identified biochemically in this work.

U73 expression in HHV-7(SB)-infected cells. RT-PCR was done to confirm that the gene encoding OBP_{H7} (U73) is expressed during lytic replication. A 133-bp amplimer was generated from RNA extracted from HHV-7(SB)-infected SupT1 cells (Fig. 2, lane 7) but not uninfected cells (lane 5). A 550-bp GAPDH product was amplified in reactions containing both uninfected and infected SupT1 RNA only upon the addition of RT (lanes 5 and 7), demonstrating the absence of DNA contamination and the presence of amplifiable RNA. The U73 primers were specific for HHV-7, since they did not produce a product with HHV-6B(Z29) DNA (lane 2).

In vitro expression of truncated OBP_{H7}. Unlike OBP_{H1}, baculovirus and bacterial expression of full-length OBP_{H6B} has yielded insoluble protein (15). As for OBP_{H6B} (14), full-length OBP_{H7} protein expressed in IVTT formed high-molecular-weight aggregates that had little binding activity by EMSA (data not shown). The carboxyl-terminal portion of OBP_{H7} (amino acids [aa] 484 to 787) closely corresponds to the smallest region of OBP_{H6B} (aa 482 to 770) required for DNA binding activity as measured by EMSA (15). The carboxyl-terminal portion of OBP_{H7} was expressed by IVTT from three plasmid constructs. From an OBP expression construct lacking a Kozak translation initiation sequence surrounding the initiating methionine, 33- and 29-kDa products were detected (Fig. 3, lane 3). The presence of a Kozak sequence resulted in higher levels of the 33-kDa protein that closely approximated the expected molecular mass of 35.4 kDa (Fig. 3, lane 4). This suggests that the smaller products initiated from internal AUG sequences. An amino-terminal FLAG-tagged OBP_{H7} fusion protein of 37 kDa was also generated that was consistent with the predicted size of 36.9 kDa (Fig. 4, lane 5). Truncated OBP_{H7} and FLAG-tagged OBP_{H7} generated from constructs containing a Kozak sequence were used in the remainder of the experiments described in this report.

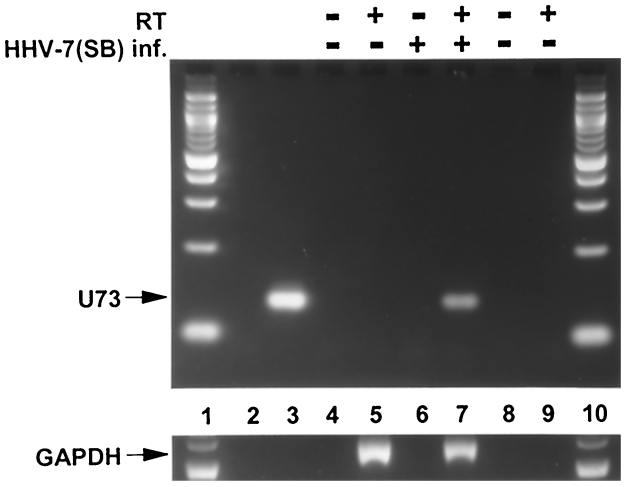

FIG. 2. RT-PCR detection of HHV-7(SB) U73 (OBP_{H7}) transcripts. Lanes 1 and 10 contain a 100-bp DNA ladder (New England Biolabs, Inc., Beverly, Mass.). Lanes 2 and 3 contain HHV-6B(Z29) and HHV-7(SB) viral nucleocapsid DNA, respectively. Lanes 4 and 5 and lanes 6 and 7 contain the PCR products of reactions with uninfected SupT1 RNA and HHV-7(SB)-infected SupT1 RNA, respectively. Lanes 8 and 9 are no-template negative controls. RT was added to lanes 5, 7, and 9. The upper and lower panels contain PCR products obtained using U73 and GAPDH primers, respectively.

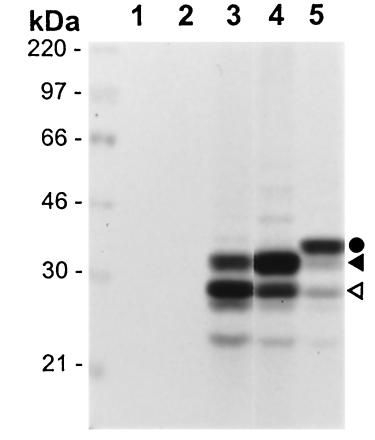

FIG. 3. In vitro expression of truncated OBP_{H7}. IVTT mixtures programmed with pCMV-Tag 2B vector DNA (lane 1), pcDNA3 with truncated U73 in the reverse orientation (lane 2), or plasmids containing the carboxyl-terminal region (aa 484 to 787) of HHV-7 U73 (lanes 3 to 5) were incubated in the presence of [^{35}S]methionine and analyzed by sodium dodecyl sulfate-polyacrylamide gel electrophoresis as described previously (14). OBP_{H7} was expressed from pcDNA3 constructs either lacking (lane 3) or containing (lane 4) a Kozak translation initiation sequence. Lane 5 contains N-terminally FLAG-tagged OBP_{H7} expressed from pCMV-Tag 2B. The circle indicates the 37-kDa FLAG-tagged OBP_{H7} fusion protein. The solid and open triangles indicate the 33- and 29-kDA products generated from constructs containing the carboxyl-terminal portion of HHV-7 U73.

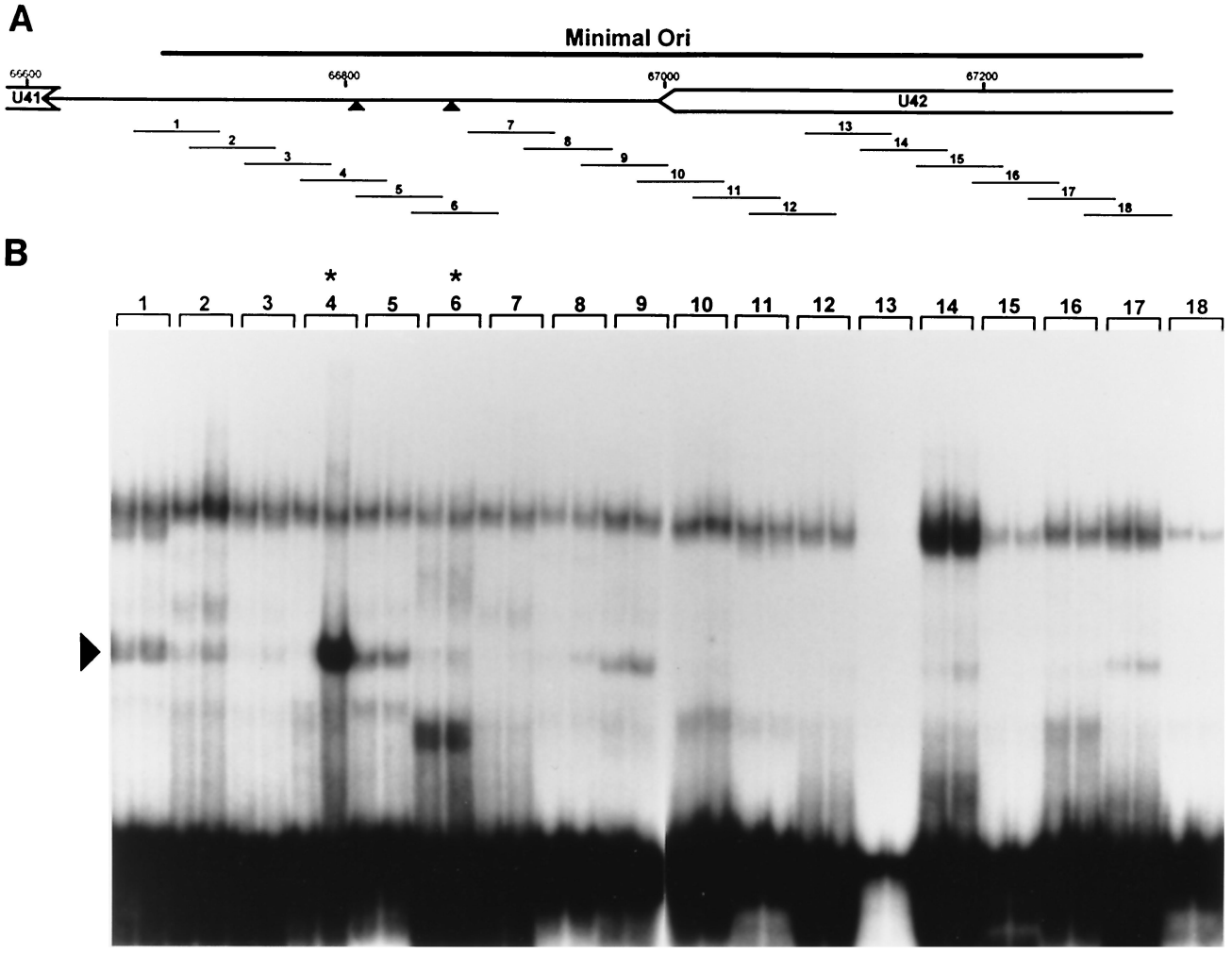

FIG. 4. Identification of an OBP_{H7}-binding site in the HHV-7 *ori*Lyt. (A) Schematic diagram of the genomic location of the 600-bp HHV-7 minimal *ori*Lyt region (27). The triangles indicate the putative HHV-7 OBP-2 and OBP-1 sites. (B) The 18 double-stranded 55-bp oligonucleotides (1 to 18) shown in panel A were used for EMSA. ^{32}P-labeled oligonucleotides were reacted with IVTT lysate programmed with truncated U73 in the reverse orientation (negative control, left lane for each oligonucleotide) or with truncated U73 in the correct forward orientation (right lane for each oligonucleotide). Asterisks indicate oligonucleotides with the putative OBP-2 and OBP-1 sites. Oligonucleotide 13 labeled inefficiently to lower specific activity; no specific binding was detected upon long exposure or by PhosphorImager analysis (data not shown). The arrowhead indicates the complex generated in the presence of oligonucleotide 4 and OBP_{H7}-containing IVTT.

The high-affinity OBP_{H7} site in the HHV-7 *ori*Lyt is identical to the HHV-6 OBP-2 site. In preliminary EMSA experiments, we found that OBP_{H7} recognized an oligonucleotide containing the putative HHV-7 OBP-2 site (data not shown). The reaction buffer used in the initial experiments (buffer B) was previously identified as optimal for OBP_{H6B} (14). Subsequent titrations indicated that higher NaCl and $MgCl_2$ concentrations (125 mM NaCl and 5 mM $MgCl_2$) were required for optimal OBP_{H7} binding (buffer A); these binding conditions were used in the following series of experiments.

Twenty-one sites in the minimal HHV-7 *ori*Lyt have at least seven of nine matches to the OPB_{H6B} consensus sequence, YGWYCWCCY. To perform an unbiased biochemical search for all OBP sites, 18 overlapping 55-bp DNA duplexes that span the 600-bp *ori*Lyt region were examined for OBP_{H7} binding (Fig. 4A). Since the IVTT expression system contains a multitude of reticulocyte proteins that may interact with the DNA targets, we included a negative control lysate in parallel with the OBP_{H7}-containing lysate for each oligonucleotide examined. The experiment was performed in duplicate, and shifts were quantitated by PhosphorImager analysis. As shown in Fig. 4B, oligonucleotide 4 was the only target that reproducibly generated a >2-fold difference in any shift pattern between the OBP_{H7}-containing lane and the negative control lane. Oligonucleotide 4 contains a 9-bp sequence identical to the HHV-6 OBP-2 site. Maintenance of this sequence is required for HHV-7 *ori*Lyt-mediated plasmid replication (27). No OBP_{H7}-specific binding was detected to oligonucleotide 6, which contains a sequence with seven of nine matches to the OBP_{H6B} consensus recognition sequence and is located on the flank of an AT-rich element opposite from the OBP-2 site. Because of the correspondence of sequence and context between this site and the HHV-6 OBP-1 site, we had expected recognition of oligonucleotide 6 by OBP_{H7} in the direct binding analysis. We

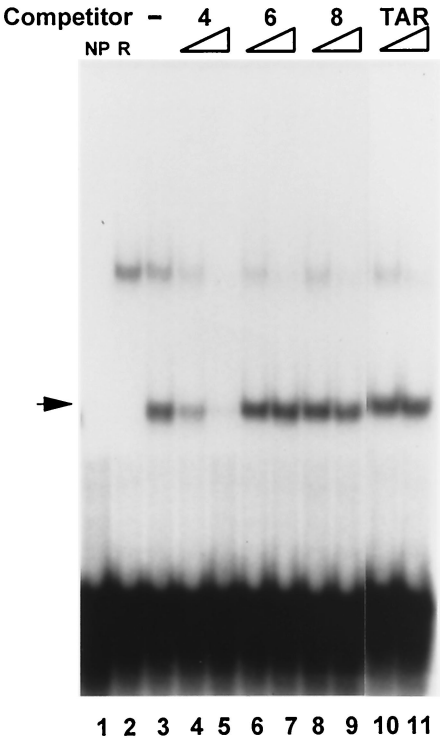

FIG. 5. Specificity of the OBP_{H7} protein–OBP-2 DNA interaction by competitive EMSA. OBP_{H7} binding to oligonucleotides 4, 6, and 8 (Fig. 4) was analyzed in competition analysis. Sixteen- and 80-fold molar excesses of the oligonucleotides were added as competitors for binding to labeled oligonucleotide 4. Oligonucleotide 8 and TAR are double-stranded oligonucleotides with no sequence similarity to an OBP site. NP, no protein added to the binding reaction; R, binding reaction contained protein from an IVTT reaction mixture programmed with a plasmid containing HHV-7 U73 in the reverse orientation; −, no competitor present; arrow, the specific shift with OBP_{H7}.

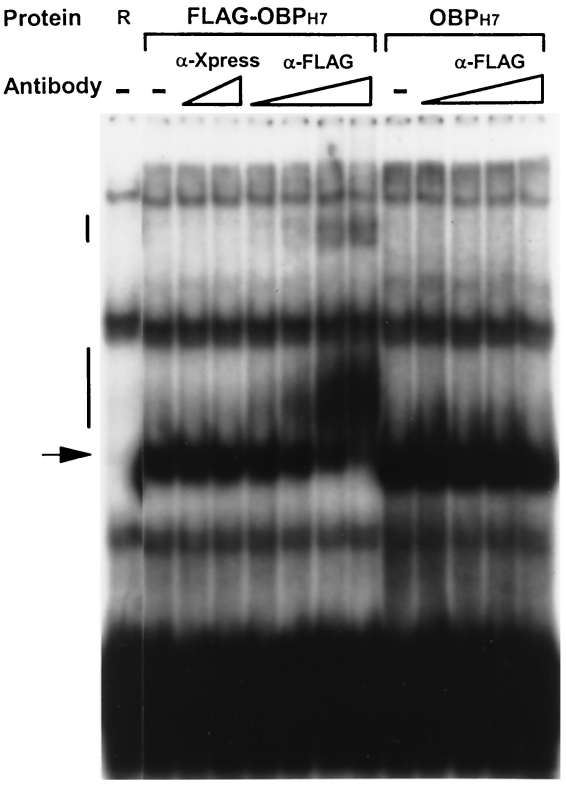

FIG. 6. Specificity of the OBP_{H7} protein–OBP-2 DNA interaction by supershift. OBP_{H7} was incubated with increasing amounts of MAbs against the Xpress (Invitrogen) or FLAG (Stratagene) epitope before the addition of the labeled 7–2 oligonucleotide (see Fig. 7C) containing the HHV-7 OBP-2 site. The triangles below α-Xpress indicate 97.6 pg and 6.25 ng of input IgG MAb. The triangles below α-FLAG indicate the addition of 97.6 pg, 0.391 ng, 1.58 ng, and 6.25 ng of IgG MAb. −, no antibody added; R, negative control lysate; arrow, the specific shift with OBP_{H7} protein; vertical bars, the supershifted complexes.

sought to confirm the results from oligonucleotides 4 and 6 in a competition analysis.

As shown in Fig. 5, only oligonucleotide 4, which contains the putative OBP-2 site, competed for binding to OBP_{H7} with labeled oligonucleotide 4. There was no evidence for recognition of oligonucleotide 6 (which contains the putative OBP-1 site) or oligonucleotide 8 and TAR (no OBP site similarity). These results confirm the specificity of the OBP-2 site interaction and demonstrate that there is a single high-affinity site for OBP_{H7} (designated OBP-2) in the HHV-7 *ori*Lyt.

OBP_{H7} is present in the specific shifted complex. To verify that the specific shifted complex contained OBP_{H7}, we did an antibody supershift experiment. A truncated OBP_{H7} protein with an amino-terminal FLAG epitope was reacted with oligonucleotide 7–2 (see Fig. 7C) in the presence of specific and nonspecific antibodies. The 50-bp 7–2 is similar to the 55-bp oligonucleotide 4 except the OBP-2 site is in a slightly different location in relation to the flanking sequence. As shown in Fig. 6, in the absence of added antibodies, both FLAG-OBP_{H7} and OBP_{H7} generated protein-DNA complexes with similar mobilities. DNA-protein complexes containing FLAG-OBP_{H7} were recognized by the antibody against the FLAG epitope to generate tertiary supershifted complexes. This antibody did not affect the mobility of DNA complexes containing OBP_{H7} protein that lacked the FLAG epitope. The specificity of this interaction was further demonstrated by the absence of a higher-mobility product upon addition of antibody of the same immunoglobulin G (IgG) subclass (IgG1) against an epitope (Xpress) not present in the OBP proteins. This experiment also demonstrates that the other shifts seen are due to interactions with other proteins of the reticulocyte lysate and are not the specific shifts of interest involving OBP_{H7}.

The OBP_{H7} minimal recognition element. The following series of experiments was intended to define the boundaries of the minimal OBP_{H7} recognition element. Three sets of shorter oligonucleotides derived from the 50-bp 7–2 oligonucleotide were generated and examined for their ability to bind OBP_{H7}. The first set of overlapping 34-bp oligonucleotides (7–2A, -B, and -C) (Fig. 7C) collectively spans the 50-bp region. In both direct binding and competition experiments, 7–2B and 7–2C were strongly bound by OBP_{H7} while 7–2A reacted only weakly (Fig. 7A and B). These results indicate that the 8-bp sequence to the right of the 7–2A boundary is not essential for recognition but does influence binding efficiency. A second set of overlapping 20-bp DNA duplexes that span 7–2B was then

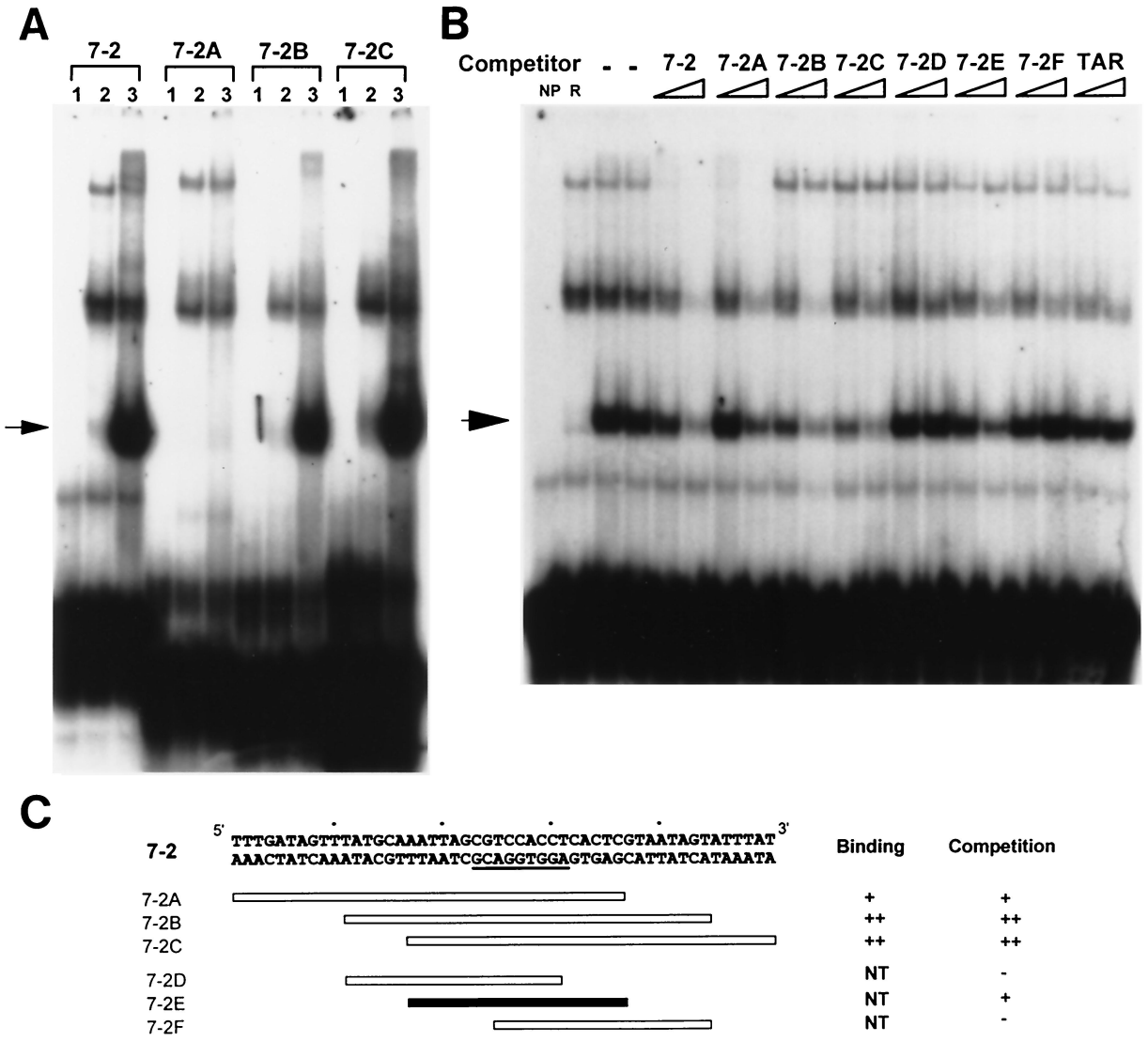

FIG. 7. Mapping the OBP-2-binding site. (A) Oligonucleotides that span the 50-bp 7–2 oligonucleotide that contains the OBP-2 site were tested for their ability to be directly bound by OBP_{H7}. For each oligonucleotide target, lane 1 contains a binding reaction mixture without any reticulocyte lysate, lane 2 contains reverse negative control lysate, and lane 3 contains lysate with truncated OBP_{H7} protein. (B) Competition EMSA with unlabeled oligonucleotides at 16- and 80-fold molar excess. −, no competitor was added. NP and R are negative controls as described in the Fig. 5 legend. In panels A and B, arrows point to the specific shifts. (C) Schematic diagram of oligonucleotides used and summary of binding and competition assay results shown in panels A and B. NT, not tested. ++ indicates a stronger degree of interaction of an oligonucleotide with OBP_{H7} than +; −, no competition observed.

tested for competition against labeled 7–2 (Fig. 7B); as summarized in Fig. 7C, only 7–2E competed.

Finally, a third panel of oligonucleotides was generated that contained variable amounts of native sequence flanking either the left or right side of the 9-bp HHV-7 OBP-2 sequence that is identical to the HHV-6B OBP-2 site. These oligonucleotides were tested for their ability to compete with labeled 7–2B for binding to OBP_{H7}. In these experiments, the amount of radioactivity in each shifted band was quantitated and is presented as the percentage of binding inhibition relative to that of a full-length control, oligonucleotide L6R7, as described in Materials and Methods. The oligonucleotides and competition results are summarized in Table 1. The shortest oligonucleotide that competed for binding was the 14-bp L0R5 oligonucleotide. This defines the minimal recognition sequence as a 14-bp element consisting of the 9-bp OBP-2 sequence plus five bases flanking to its right.

The OBP_{H7} and the OBP_{H6B} consensus recognition sequences are closely related. The consensus recognition sequence for a DNA binding protein is a powerful tool for understanding the basis of sequence specificity for a protein-DNA interaction. In addition, comparison of the consensus sequences among OBPs enables an evaluation of their evolutionary divergence. To determine the OBP_{H7} consensus recognition sequence, we used the saturation mutagenesis technique described previously for OBP_{H6B} (15) and OBP_{H1} (13). We designed a panel of double-stranded oligonucleotides that contained all possible single base pair substitutions at each

TABLE 1. Oligonucleotides used for EMSA

Competitor	Sequence	Length (bp)	Binding inhibition (%)[a]
	AATTAGCGTCCACCTCACTCGT		
L6R7	**********	22	100
L5R6	**********	20	100
L4R5	**********	18	89
L3R4	**********	16	0
L2R3	**********	14	0
L1R2	**********	12	0
L0R1	**********	10	0
L3R6	**********	18	100
L3R5	**********	17	100
L2R5	**********	16	100
L1R5	**********	15	100
L0R5[b]	**********	14	76
L5R4	**********	18	47
L4R4	**********	17	28
L4R3	**********	16	0
L4R2	**********	15	0
L4R1	**********	14	0

[a] The percentage inhibition of radiolabeled oligonucleotide 7–2B binding to truncated OBP_{H7}, relative to the inhibition from oligonucleotide L6R7.

[b] L0R5 is the smallest oligonucleotide that competes for OBP_{H7} recognition.

position of the 14-bp minimal recognition element; 60-fold molar excesses of these oligonucleotides were then tested for their ability to compete with 7–2B for binding to OBP_{H7}. The effect of each substitution was determined by quantifying the radioactivity of the shifted band and expressing this value as the percentage of binding inhibition relative to that of the wild-type 7–2E or 7–2Eext oligonucleotide.

A representative set of the competition experiments is presented in Fig. 8A. Mutated oligonucleotides such as M2T (substitution with a thymidine at position 2), which contained a substitution that resulted in <70% inhibition of binding compared to the wild-type oligonucleotide, were considered to have a nonpermissive substitution. Mutated oligonucleotides such as M2A (Fig. 8A), which retained its ability to compete for binding (>70%) as compared to that of the wild-type oligonucleotide, contained a permissive base pair. Designation as a permissive or nonpermissive change was based on quantitative trends observed in at least three independent experiments. The results of these experiments are summarized in Fig. 8B and allow deduction of the OBP_{H7} consensus sequence, BRTYCWCCT.

OBP_{H7} tolerates less sequence variation from positions 2 through 9 (Fig. 8B). While there was some degree of sequence preference at positions 10 through 14, the gradient was so slight that a consensus sequence could not be determined. In comparison with the OBP_{H6B} consensus at positions 1 and 2, the OBP_{H7} consensus recognition sequence is more permissive. At positions 3 and 9 there was overlap with the OBP_{H6B} consensus, but OBP_{H7} is less permissive than OBP_{H6B}. From the consensus sequences for OBP_{H6B} and OBP_{H7}, YCWCC was identified as the central core sequence for roseolovirus OBP recognition, in comparison to the C—C core shared with OBP_{H1} and the other alphaherpesviruses. The OBP-2 site and the putative OBP-1 site are the only sites in the HHV-7 *ori*Lyt that exactly match the experimentally derived OBP_{H7} consensus sequence.

Identification of OBP-1 as a low-affinity binding site. As described above, the only sites in the HHV-7 *ori*Lyt that exactly match the OBP_{H7} consensus sequence are the OBP-2 site we identified in the previous mapping experiments and the putative OBP-1 site, which is in a position and context that suggest its possible function as an OBP-binding site. Because oligonucleotides containing the putative OBP-1 site were not recognized in any of the preceding experiments, we examined the effect of different buffer conditions on DNA binding activity. As measured by signal intensity in the absence of competitor, the ability of OBP_{H7} to bind an oligonucleotide that contains the OBP-2 site, 7–2B, was reduced 10-fold in buffer B (the buffer optimized for OBP_{H6B}) (14) compared to buffer A (the buffer optimized for OBP_{H7}), but the protein-DNA interactions were concomitantly altered to allow binding to the 34-bp 7–1B oligonucleotide that contained the OBP-1 sequence (Fig. 9). As shown in Fig. 9B, a second oligonucleotide that contained the OBP-1 sequence, the 55-bp oligonucleotide 6 (Fig. 4A), was also bound by OBP_{H7} in buffer B. This reactivity was not due to a loss of specificity in buffer B conditions, since the nonspecific TAR oligonucleotide does not compete for binding to OBP_{H7} (Fig. 9B) and the oligonucleotide M3A, which contains a single nonpermissive mutation, was not recognized (data not shown). OBP_{H7} had a higher affinity for oligonucleotides containing the OBP-2 site than for those containing the OBP-1 site in both binding conditions.

Heteroduplex analysis suggests that OBP_{H7} interacts with one face of the DNA helix. To identify the strand-specific base interactions required for OBP_{H7} recognition of the high-affinity OBP-2 site, we generated heteroduplex oligonucleotides derived from the 7–2E sequence (Fig. 7C) that contain single mismatched base pairs at positions 2 through 9. The heteroduplex oligonucleotides and corresponding oligonucleotides with complementary substitutions on both strands (nonheteroduplex) were compared for their ability to compete for binding against the wild-type sequence in oligonucleotide 7–2E. Sense strand alterations at positions 2, 3, 4, and 9 as well as complementary strand alterations at positions 5 through 8 resulted in loss of recognition by OBP_{H7} at levels similar to or greater than alterations on both strands at these positions (Fig. 10A). Changes on the opposite strand at these positions resulted in at least a threefold-greater inhibition of binding than the alteration on both strands, indicating that the principal interaction is not on this strand at this position. For example, when both strands (Fig. 10A, lane b) at position 2 were changed from a GC to a TA base pair, the resulting oligonucleotide did not compete for binding. A sense strand changed to a T at position 2 (lane sT) was also unable to compete; this is in contrast to the effect of a complementary strand change to an A (lane cA), which competes as well as the wild-type sequence. This indicates that the base on the sense strand of the oligonucleotide at position 2 is a possible contact point for OBP_{H7}.

The strand-specific alterations that resulted in loss of recognition and thus are considered possible points of contact with OBP_{H7} are summarized in Fig. 10B and C. In the helical wheel representation of the OBP-2 sequence, the side of the DNA helix that is critical for recognition is found along one face (Fig. 10B). In a simulation of the OBP-2 site as B-form DNA,

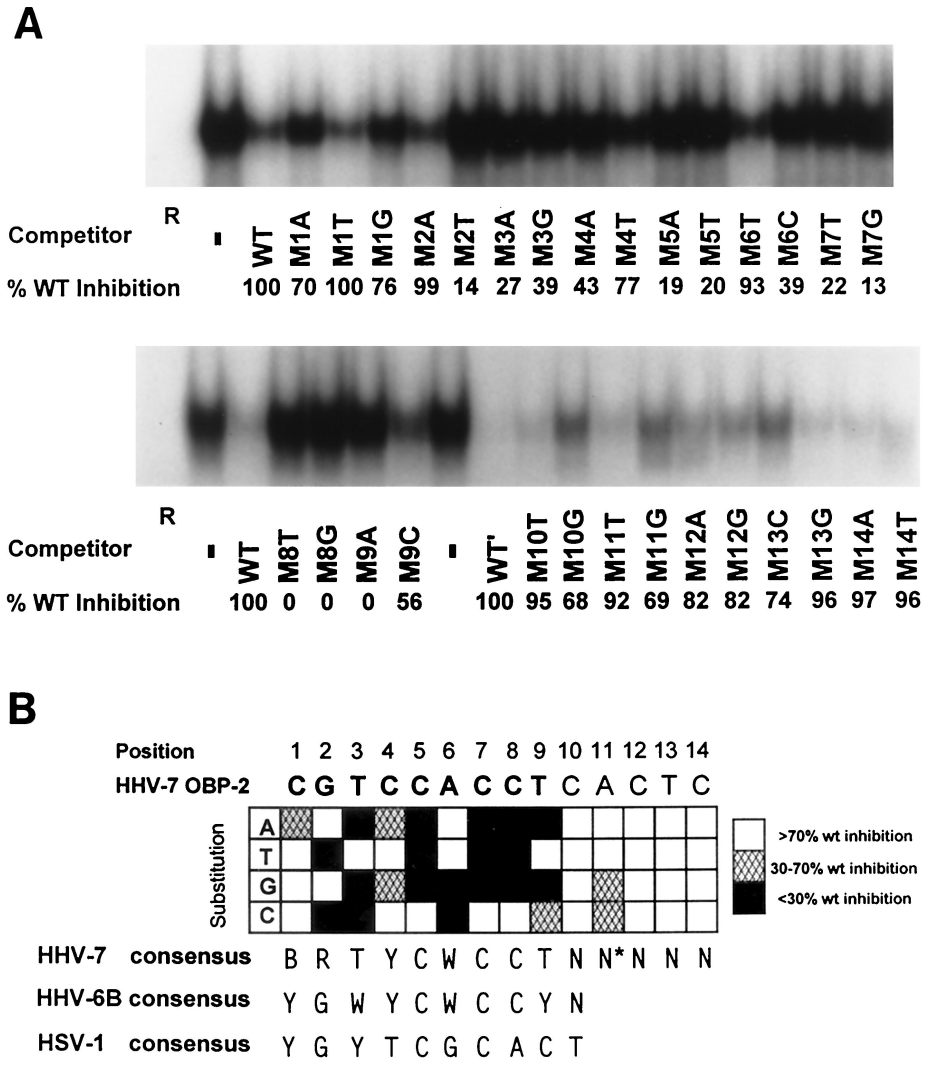

FIG. 8. Effect of substitutions in the 14-bp core OBP-2 sequence and the resulting OBP_{H7} consensus recognition sequence. (A) Saturation mutagenesis of the minimal OBP_{H7} recognition sequence (Table 1, oligonucleotide L0R5). At each position of the 14-bp minimal recognition sequence, oligonucleotides were generated that contained changes to the other three possible base pairs. The label beneath each lane of the gel indicates the position and change made in the competitor used. Sixty-fold molar excesses of unlabeled mutated oligonucleotides were used in competitive EMSA against ^{32}P-labeled 7–2B. The amount of residual shifted radioactivity after competition was quantified by PhosphorImager analysis (Molecular Dynamics). The inhibition of binding of ^{32}P-labeled 7–2B DNA to truncated OBP_{H7} by each competitor DNA duplex is shown beneath the gel as the percent inhibition relative to the wild-type DNA duplex (WT). The other competitor DNA duplexes shown in panel B were analyzed similarly (data not shown). Positions 10 to 14 were analyzed in the context of the sequence of the longer 7–2Eext oligonucleotide, AATTAGCGTCCACCTCACTCGTAATAGT (WT′), to avoid effects that might be more dependent on proximity to the end of the oligonucleotide than sequence alone. −, no competitor was added. (B) Summary of saturation mutagenesis and the resulting consensus recognition sequence. Open blocks indicate that the given alteration at that position did not result in loss of recognition (competition was at least 70% of WT) and is therefore a permissive change. Hatched and solid blocks indicate that the alteration reduced the binding ability partially or severely, respectively. These designations were based on quantitative trends observed in at least three independent experiments. The asterisk on the N at position 11 indicates that although two of the changes were slightly below the cutoff for recognition, the slight gradient in recognition of all alterations at this position did not enable identification of a clearly preferred sequence. In the consensus sequence, B is a T, G, or C; R is a G or A; Y is a T or C; W is a T or A; and N is any nucleotide.

7 of the 8 potential points of contact in the core recognition element examined in Fig. 10A are present in the major groove (Fig. 10C). These results indicate that OBP_{H7} may interact with the core of its OBP site in the major groove along one face of the DNA helix. Position 9 lies outside the major groove, but along the same face, and may reflect possible phosphate interactions that are disrupted by a strand mismatch.

DISCUSSION

We have characterized the interaction of OBP_{H7} with the HHV-7 *ori*Lyt. As with alphaherpesviruses, this is likely the first step in a cascade of events required for initiation of viral replication. Specifically, we determined that (i) the carboxyl-terminal 304 aa are sufficient for DNA binding activity, (ii)

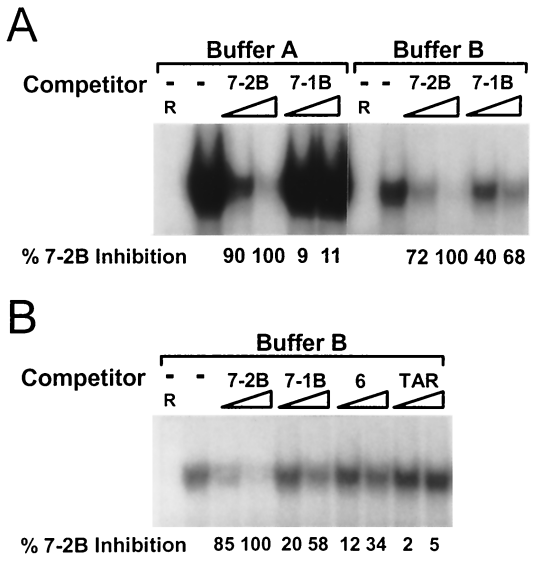

FIG. 9. Identification of a second, lower-affinity OBP site (OBP-1) by competitive EMSA. (A) Competition with 16- and 80-fold molar excesses of unlabeled DNA duplexes containing HHV-7 OBP-2 (7–2B) and OBP-1 (7–1B, GGAGGGTTCATTGATCCTCCTTGCCTGCAA TTCT) with ^{32}P-labeled 7–2 for binding to OBP_{H7} in buffers A and B (see Materials and Methods). The amount of residual shifted target was quantitated by PhosphorImager analysis. The percentage of inhibition of binding to ^{32}P-labeled 7–2 DNA relative to 7–2B at 80-fold molar excesses by each competitor DNA duplex is shown beneath the gel. −, no competitor present; R, negative control lysate. (B) Conditions are the same as described for panel A, except that binding buffer B was used. Oligonucleotide 6 contains the OBP-1 site and is described in the legend to Fig. 4. TAR is described in the legend for Fig. 5.

there are two binding sites with markedly different affinities for OBP_{H7} in the HHV-7 *ori*Lyt, (iii) BRTYCWCCT is the OBP_{H7} consensus recognition sequence, and (iv) strand-specific interactions in the 9-bp OBP core occur along one face of the DNA helix.

OBP_{H7} sequence recognition. The minimal OBP_{H7} recognition element is 14 bp in length, similar to the 13-bp minimal element of OBP_{H6B} (15) and the 15-bp element of OBP_{H1} (13). For both OBP_{H6B} and OBP_{H7}, additional sequence was required on the right flank of the 9-bp core recognition sequence, suggesting that the flanking sequence is required to stabilize the protein-DNA interaction. The roseolovirus OBPs have identical sequence specificity in the central 5-bp region of the 9-bp recognition core (YCWCC); outside the 5-bp region, their specificity diverges. This difference in specificity does not appear to have been substantially influenced by differences in the buffers used during determination of the consensus sequences (data not shown). For both viruses, the consensus sequences are consistent with the authentic OBP-1 sites. Ultimate proof would require evaluation of these sequences under physiologic conditions such as transient replication assays.

Using the OBP_{H7} consensus recognition sequence to search the genomes of HHV-7 strains JI (23) and RK (22) for exact matches, we identified 11 potential OBP sites in addition to the 2 identified in the HHV-7 *ori*Lyt in both genomes. Three are present in each copy of the genome-bounding direct repeat elements (a total of six copies per genome), with the remaining sites scattered in the unique segment. None of the sequences is linked to another in a manner suggestive of an authentic origin region.

Like OBP_{H6B} (15) and OBP_{H1} (13, 25), OBP_{H7} required strand-specific base interactions within the OBP recognition core that align along one face of the DNA helix in the major groove. These results are consistent with the higher-resolution model for OBP_{H1}, in which an alpha helix in its carboxyl-terminal DNA binding domain fits into the major groove to mediate specific base contacts at an OBP site (9, 13, 25).

Unlike OBP_{H6B}, which recognizes both OBP sites in the HHV-6 *ori*Lyt with comparable affinities, OBP_{H7} has a higher affinity for OBP-2 than OBP-1. The OBP-1 site fits the OBP_{H7} consensus sequence, yet there are three differences in the 9-bp core between OBP-1 (GATCCTCCT) and OBP-2 (CGTCCA CCT). In competition experiments utilizing a buffer (buffer A) in which the OBP-2 site is bound strongly while OBP-1 is not detectably bound, there was a progressive decrease in binding to oligonucleotides that contained various combinations of the OBP-1-derived sequence (data not shown). This indicates that the differences in the 9-bp recognition core compound to create an overall low-affinity OBP-1 site.

Mutated OBP_{H1} binding sites that are not individually bound in vitro have less of an impact on binding by full-length OBP_{H1} in the context of the entire ori_S (9). This cooperativity is ablated upon disruption of the amino-terminal multimerization domain of OBP_{H1} (12). Truncated OBP_{H7} recognized OBP-1 and OBP-2 with markedly different affinities, suggesting that cooperative interactions through multimerization of full-length OBP_{H7} may be required at the OBP sites in the HHV-7 *ori*Lyt. Protein-protein interactions with OBP_{H7} bound to the high-affinity OBP-2 site may increase the stability of an OBP complex at the low-affinity OBP-1 site. Unlike OBP_{H7}, OBP_{H6B} binds its two sites with comparable affinities. This indicates that OBP protein-DNA interactions differ between OBP_{HB6} and OBP_{H7}.

Comparison of the OBP-binding regions of roseoloviruses and alphaherpesviruses. The HHV-7 *ori*Lyt has features conserved in the lytic origin regions of alphaherpesviruses and of HHV-6A and HHV-6B (Fig. 11). Like HHV-6A and HHV-6B, the HHV-7 AT-rich spacer region is longer than in alphaherpesvirus *ori* regions and has imperfect dyad symmetry. Unlike the other origin regions shown here, the AT-rich spacer element in HHV-7 contains few AT repeats.

Interestingly, the HHV-7 *ori*Lyt contains a sequence that has a 9-of-12 match with the HSV Box III element and a 6-of-9 match with the OBP_{H7} consensus recognition sequence; a similar sequence is not present in the HHV-6A and HHV-6B *ori*Lyts. This element is found in a position in HHV-7 that corresponds to its location in HSV, that is, immediately to the left of the Box I site. Mutations in Box III decrease the replication of an ori_S-containing plasmid in transient replication assays (19). However, the HSV Box III site is detectably bound only in the context of cooperative binding of full-length OBP_{H1} to an ori_S segment containing the Box I and II sites (9, 10). Recent data suggest that Box I and III may interact to form a secondary structure through a 6-bp region of dyad symmetry in ori_S that is required for stable interaction with OBP_{H1} (3). There is also an element of dyad symmetry (5 bp) between HHV-7 OBP-1 and its Box III-like site.

The OPB-1 site-containing oligonucleotides 6 and 7–1B both

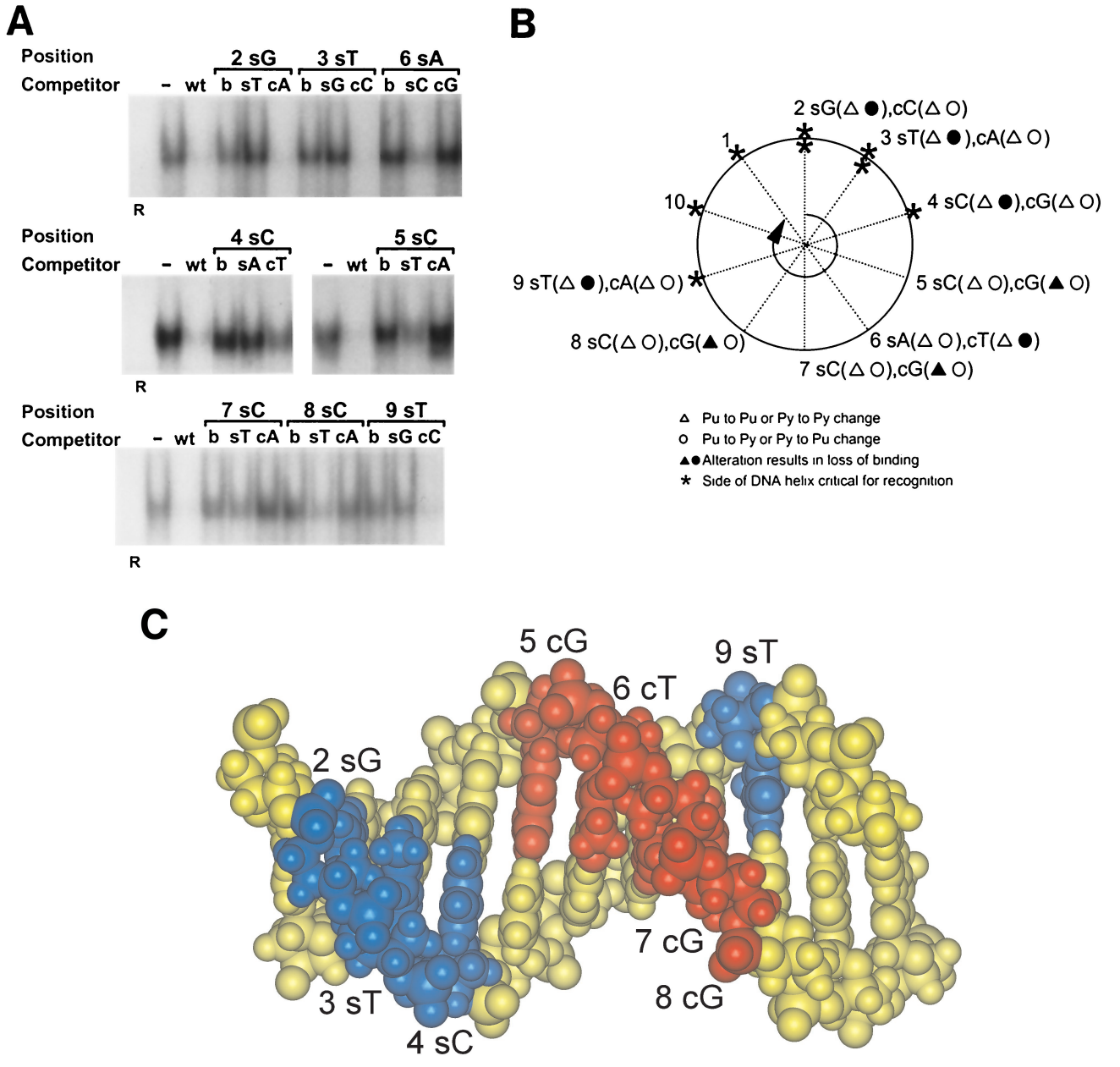

FIG. 10. EMSA to measure recognition of heteroduplexes. (A) Heteroduplex oligonucleotides containing single mismatched base pairs at positions 2 through 9 were created by annealing a wild-type 7–2Eext oligonucleotide to complementary oligonucleotides containing single nucleotide substitutions. For positions 2 through 9, 60-fold molar excesses of heteroduplex oligonucleotides with a mutation on the 5′-to-3′ sense strand (s) or a mutation of the 3′-to-5′ complementary strand (c) were compared for their ability to compete for binding with truncated OBP_{H7} against oligonucleotides containing the mutation on both strands (b). −, no competitor; WT, wild-type 7–2E is the competitor; R, negative control protein lysate. (B) Helical wheel representation of heteroduplex analysis. The 9-bp OBP-2 core sequence is arranged on a helical wheel to approximate the 10.4 base residues per turn of a B-form DNA helix. For each position, two heteroduplex oligonucleotides were synthesized with changes on the sense strand (first set of parentheses) and two were made with changes on the complementary strand (second set of parentheses). Purine-to-purine and pyrimidine-to-pyrimidine changes are indicated by triangles. Purine-to-pyrimidine and pyrimidine-to-purine changes are indicated as circles. Solid symbols indicate that strand-specific alteration is responsible for loss of recognition at that position in the core sequence. Asterisks indicate the side of the DNA helix that is critical for recognition; thus, a change on the complementary strand that affects recognition is indicated by an asterisk on the opposite side of the helix (e.g., the T at position 6). (C) A B-form DNA model of the OBP-2 site, CGTCCACCTCA, was produced using Insight II, Release 2000 (Molecular Simulations, Incorporated, San Diego, Calif.). Labeled positions indicate strand mismatches that resulted in the loss of recognition by OBP_{H7}.

had comparable affinities for OBP_{H7}, but only oligonucleotide 6 contains the Box III-like site. Further analysis of the interaction of full-length OBP_{H7} with oligonucleotides containing mutations in the Box III site is required to determine what impact it may have on recognition of the flanking OBP-1 site. HHV-7-infected cells replicated an HHV-6 *ori*Lyt-containing plasmid (27), and the HHV-6 *ori*Lyt region lacks the 12-bp HSV Box III-like site found in the HHV-7 *ori*Lyt. This suggests

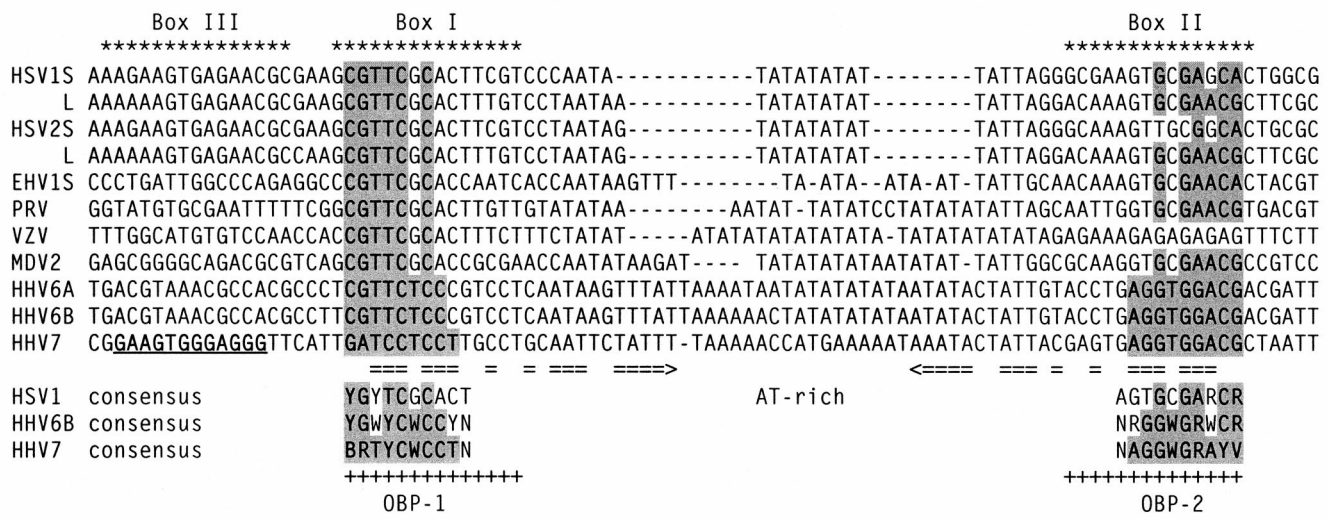

FIG. 11. Comparison of the OBP sites in the *ori* regions of alphaherpesviruses and roseoloviruses. OBP-binding regions of the *ori*Lyts of alphaherpesviruses and roseoloviruses are shown. HSV1 L, HSV-1 ori_L; HSV1 S, HSV-1 ori_S; HSV2 L, HSV-2 ori_L; HSV2 S, HSV-2 ori_S; EHV1 S, equine herpesvirus 1 ori_S; PRV, pseudorabies virus; VZV, varicella-zoster virus; MDV2, Marek's disease virus 2; I, II, and III, Box I, II, and III of HSV-1 ori_S. Residues that match the HHV-7 consensus are shaded. Horizontal arrows indicate a structure with dyad symmetry in the HHV-7 sequence. The HHV-7 Box III-like sequence is underlined.

that the Box III-like element is probably not essential for possible cooperative interactions of OBP_{H7} at the origin of replication by other HHV-7 replication factors.

Differences in the interaction of roseolovirus OBPs with their *ori*Lyts. OBP_{H7} and OBP_{H6B} have similarities in their DNA binding properties, namely, that their consensus recognition sequences overlap and they recognize an identical 9-bp element in their *ori*Lyt regions. However, in transient replication-infection assays, the HHV-7 replication machinery replicated an HHV-6 *ori*Lyt-containing plasmid while an HHV-7 *ori*Lyt-containing plasmid did not replicate in HHV-6B-infected cells (27). The basis for the lack of reciprocity may simply lie in differences in sequence recognition between OBP_{H6B} and OBP_{H7}: the 9-bp core of the HHV-6B OBP-1 site differs by a single base from the OBP_{H7} consensus recognition sequence while the HHV-7 OBP-1 site and OBP_{H6B} consensus sequence differ at two positions. This interaction could be further affected by differences in proximal flanking sequences. In addition, as described above, the HHV-7 *ori*Lyt lacks the long IDRs and putative DNA unwinding element of the HHV-6 *ori*Lyts but contains a putative Box III-like element. The sum of these differences within and around the OBP sites is likely to affect OBP_{H6B} and OBP_{H7} activities in the *ori*Lyts.

Much can be learned about the mechanism of DNA replication initiation of roseoloviruses from a comparative functional analysis of their closely related, yet distinct, OBP proteins. We are presently studying reciprocity at the level of DNA binding between the OBPs and OBP sites of HHV-6 and HHV-7.

ACKNOWLEDGMENTS

L.T.K. was supported in part through an appointment to the Research Participation Program at the Centers for Disease Control and Prevention administered by the Oak Ridge Institute for Science and Education.

We thank Elizabeth Neuhaus for constructing the DNA model, Felicia Stamey for sequencing the OBP constructs, the CDC Biotechnology Core Facility for oligonucleotide synthesis, and James Gathany for photography.

REFERENCES

1. **Anders, D. G., M. A. Kacica, G. Pari, and S. M. Punturieri.** 1992. Boundaries and structure of human cytomegalovirus *ori*Lyt, a complex origin for lytic-phase DNA replication. J. Virol. **66:**3373–3384.
2. **Anders, D. G., and S. M. Punturieri.** 1991. Multicomponent origin of cytomegalovirus lytic-phase DNA replication. J. Virol. **65:**931–937.
3. **Aslani, A., S. Simonsson, and P. Elias.** 2000. A novel conformation of the herpes simplex virus origin of DNA replication recognized by the origin binding protein. J. Biol. Chem. **275:**5880–5887.
4. **Black, J. B., D. A. Burns, C. S. Goldsmith, P. M. Feorino, K. Kite-Powell, R. F. Schinazi, P. W. Krug, and P. E. Pellett.** 1997. Biologic properties of human herpesvirus 7 strain SB. Virus Res. **52:**25–41.
5. **Black, J. B., and P. E. Pellett.** 1999. Human herpesvirus 7. Rev. Med. Virol. **9:**245–262.
6. **Boehmer, P. E., and I. R. Lehman.** 1997. Herpes simplex virus DNA replication. Annu. Rev. Biochem. **66:**347–384.
7. **Dewhurst, S., S. C. Dollard, P. E. Pellett, and T. R. Dambaugh.** 1993. Identification of a lytic-phase origin of DNA replication in human herpesvirus 6B strain Z29. J. Virol. **67:**7680–7683.
8. **Dewhurst, S., D. M. Krenitsky, and C. Dykes.** 1994. Human herpesvirus 6B origin: sequence diversity, requirement for two binding sites for origin-binding protein, and enhanced replication from origin multimers. J. Virol. **68:**6799–6803.
9. **Elias, P., C. M. Gustafsson, and O. Hammarsten.** 1990. The origin binding protein of herpes simplex virus 1 binds cooperatively to the viral origin of replication oris. J. Biol. Chem. **265:**17167–17173.
10. **Elias, P., C. M. Gustafsson, O. Hammarsten, and N. D. Stow.** 1992. Structural elements required for the cooperative binding of the herpes simplex virus origin binding protein to oriS reside in the N-terminal part of the protein. J. Biol. Chem. **267:**17424–17429.
11. **Gompels, U. A., J. Nicholas, G. Lawrence, M. Jones, B. J. Thomson, M. E. Martin, S. Efstathiou, M. Craxton, and H. A. Macaulay.** 1995. The DNA sequence of human herpesvirus-6: structure, coding content, and genome evolution. Virology **209:**29–51.
12. **Hazuda, D. J., H. C. Perry, and W. L. McClements.** 1992. Cooperative interactions between replication origin-bound molecules of herpes simplex virus origin-binding protein are mediated via the amino terminus of the protein. J. Biol. Chem. **267:**14309–14315.
13. **Hazuda, D. J., H. C. Perry, A. M. Naylor, and W. L. McClements.** 1991. Characterization of the herpes simplex virus origin binding protein interaction with oris. J. Biol. Chem. **266:**24621–24626.
14. **Inoue, N., T. R. Dambaugh, J. C. Rapp, and P. E. Pellett.** 1994. Alphaherpesvirus origin-binding protein homolog encoded by human herpesvirus 6B, a betaherpesvirus, binds to nucleotide sequences that are similar to *ori* regions of alphaherpesviruses. J. Virol. **68:**4126–4136.

15. **Inoue, N., and P. E. Pellett.** 1995. Human herpesvirus 6B origin-binding protein: DNA-binding domain and consensus binding sequence. J. Virol. **69:**4619–4627.
16. **Lawrence, G. L., J. Nicholas, and B. G. Barrell.** 1995. Human herpesvirus 6 (strain U1102) encodes homologues of the conserved herpesvirus glycoprotein gM and the alphaherpesvirus origin-binding protein. J. Gen. Virol. **76:**147–152.
17. **Lee, S. S., and I. R. Lehman.** 1999. The interaction of herpes simplex type 1 virus origin-binding protein (UL9 protein) with Box I, the high affinity element of the viral origin of DNA replication. J. Biol. Chem. **274:**18613–18617.
18. **Lindquester, G. J., J. J. O'Brian, E. D. Anton, C. A. Greenamoyer, P. E. Pellett, and T. R. Dambaugh.** 1997. Genetic content of a 20.9 kb segment of human herpesvirus 6B strain Z29 spanning the homologs of human herpesvirus 6A genes U40–57 and containing the origin of DNA replication. Arch. Virol. **142:**103–123.
19. **Martin, D. W., S. P. Deb, J. S. Klauer, and S. Deb.** 1991. Analysis of the herpes simplex virus type 1 OriS sequence: mapping of functional domains. J. Virol. **65:**4359–4369.
20. **Masse, M. J., S. Karlin, G. A. Schachtel, and E. S. Mocarski.** 1992. Human cytomegalovirus origin of DNA replication (oriLyt) resides within a highly complex repetitive region. Proc. Natl. Acad. Sci. USA **89:**5246–5250.
21. **Masse, M. J. O., M. Messerle, and E. Mocarski.** 1997. The location and sequence composition of the murine cytomegalovirus replicator (oriLyt). Virology **230:**350–360.
22. **Megaw, A. G., D. Rapaport, B. Avidor, N. Frenkel, and A. J. Davison.** 1998. The DNA sequence of the RK strain of human herpesvirus 7. Virology **244:**119–132.
23. **Nicholas, J.** 1996. Determination and analysis of the complete nucleotide sequence of human herpesvirus 7. J. Virol. **70:**5975–5989.
24. **Romi, H., O. Singer, D. Rapaport, and N. Frenkel.** 1999. Tamplicon-7, a novel T-lymphotropic vector derived from human herpesvirus 7. J. Virol. **73:**7001–7007.
25. **Simonsson, S., T. Samuelsson, and P. Elias.** 1998. The herpes simplex virus type 1 origin binding protein. Specific recognition of phosphates and methyl groups defines the interacting surface for a monomeric DNA binding domain in the major groove of DNA. J. Biol. Chem. **273:**24633–24639.
26. **Stamey, F. R., G. Dominguez, J. B. Black, T. R. Dambaugh, and P. E. Pellett.** 1995. Intragenomic linear amplification of human herpesvirus 6B *ori*Lyt suggests acquisition of *ori*Lyt by transposition. J. Virol. **69:**589–596.
27. **van Loon, N., C. Dykes, H. Deng, G. Dominguez, J. Nicholas, and S. Dewhurst.** 1997. Identification and analysis of a lytic-phase origin of DNA replication in human herpesvirus 7. J. Virol. **71:**3279–3284.
28. **Vink, C., E. Beuken, and C. A. Bruggeman.** 1997. Cloning and functional characterization of the origin of lytic-phase DNA replication of rat cytomegalovirus. J. Gen. Virol. **78:**2963–2973.
29. **Wyatt, L. S., and N. Frenkel.** 1992. Human herpesvirus 7 is a constitutive inhabitant of adult human saliva. J. Virol. **66:**3206–3209.